

# A study of spectral element method for elliptic interface problems with nonsmooth solutions in $\mathbb{R}^2$

N. Kishore Kumar<sup>‡</sup>, Pankaj Biswas<sup>†</sup> and B. Seshadri Reddy<sup>§</sup>

## Abstract

The solution of the elliptic partial differential equation has interface singularity at the points which are either the intersections of interfaces or the intersections of interfaces with the boundary of the domain. The singularities that arises in the elliptic interface problems are very complex. In this article we propose an exponentially accurate nonconforming spectral element method for these problems based on [7, 18]. A geometric mesh is used in the neighbourhood of the singularities and the auxiliary map of the form  $z = \ln \xi$  is introduced to remove the singularities. The method is essentially a least-squares method and the solution can be obtained by solving the normal equations using the preconditioned conjugate gradient method (PCGM) without computing the mass and stiffness matrices. Numerical examples are presented to show the exponential accuracy of the method.

**Key Words:** Interface, Nonsmooth solution, Geometric mesh, Auxiliary mapping, Least-Squares solution, Preconditioner.

**Mathematics Subject Classification:** 65N35, 65F08

## 1 Introduction

An interface problem is a special case of an elliptic differential equation with discontinuous coefficients. Such interface problems arise in different situations, for example, in heat conduction or in elasticity problems whose solution domains are composed of several different materials. There are different kinds of elliptic interface problems: the interface problems with smooth interfaces, the interface problems with nonsmooth solutions etc. When the interface is smooth enough the solution of the interface problem is also very smooth in the individual regions but global regularity is low, i.e the solution  $u \in H^1(\Omega)$  and  $u \notin H^k(\Omega)$  for  $k \geq 2$ . This case has been widely addressed in the literature using finite element methods [3, 4, 5], immersed interface methods [20] and least-squares methods [6] etc. For further information on this problem and existing numerical approaches in the literature, refer to [18]. In this article we consider the interface problems with nonsmooth solutions.

In the solution of the elliptic boundary value problems, singularities may occur when the boundary is not smooth [9] or when the boundary is smooth yet one or more data are not smooth. The second type of singularity typically arises in interface problems. The singularities that arises in the interface problems are very complex. The solution of the elliptic differential equation has interface singularity at the points which are either the intersections of interfaces or the intersections of interfaces with the boundary of the domain. The solution also has singular behavior at the points where the interfaces crosses each other. The interface singularity at the crossing of interfaces is very strong.

The singularities in interface problems has been studied by Kellogg (considered the interface problem for Poisson equation) in [12]. In [13] Kellogg had studied the Poisson equation with intersecting interfaces.

\*BITS-Pilani Hyderabad Campus, Hyderabad , India; Email: naraparaju@hyderabad.bits-pilani.ac.in

<sup>†</sup>This research work is supported by National Board of Higher Mathematics, DAE, India.

<sup>‡</sup>National Institute of Technology Silchar, Silchar, India, Email:pankaj@math.nits.ac.in

<sup>§</sup>BITS-Pilani Hyderabad Campus, Hyderabad

The complexity depends on the structure of the eigenvalues of Sturm-Liouville problems corresponding to the singularities. The elliptic interface problems with singularities also has been studied in [14, 22, 23].

The conventional numerical approaches (the finite difference as well as finite element) may fail to provide any practical engineering accuracy at a reasonable cost. In [3] Babuska studied the interface problem in the frame work of finite element method. The rates of convergence are algebraic for the  $h$ -version and  $p$ -version of the finite element method. The mesh refinements techniques gives reasonably good results but they require longer computing time and also cannot give acceptable result when the singularities are very strong. The method of auxiliary map has been introduced in [24] for the interface problems by Oh and Babuska in the framework of  $p$ - version of FEM (originally introduced in [21] for elliptic problems containing singularities as MAM). With a proper choice of auxiliary mappings this method gives better results than the mesh refinements when the interface singularities are very strong. An optimal choice of the auxiliary mappings requires a prior knowledge of the structure of the interface singularities at the singular points.

In [1] an exponentially accurate method ( $hp$  finite element) has been proposed by Babuska and Guo for the elliptic problems with analytic data on the nonsmooth domains like the domains with cracks, re-entrant corners. Geometric mesh has been considered near the corners to resolve the singularities in the solution. They have studied the regularity of the solution in the framework of weighted Sobolev space  $H_{\beta}^{k,2}(\Omega)$  and the countably normed space  $B'_{\beta}(\Omega)$ . In [2] Babuska and Guo have analyzed the regularity of the interface problem in terms of countably normed spaces. In [10] Guo and H. S. Oh analyzed the  $hp$  version of the finite element method for problems with interfaces. They have used geometric mesh near the singularities and shown the exponential accuracy. Geometric mesh together with the auxiliary mapping technique gives better results even if the singularities are extremely severe. They have also presented the theoretical results for interface problems. The theoretical results and numerical scheme of this version can also be applied to general elliptic equations and systems, including elasticity problems with homogeneous and non-homogeneous materials.

In [11] H. Hon and Z. Huang introduced the direct method of lines for numerical solution of interface problems. The interface problem is reduced to variational-differential (V-D) problem on semi-infinite strip in  $\rho$  and  $\phi$  variables by using a suitable transformation of coordinates. Furthermore, the V-D problem is discretized respect with the variable  $\phi$  and solved numerically. This method requires no prior knowledge of the constructure of the singularity at the singular point.

In [7, 16, 17] P. Dutt et. al. proposed an exponentially accurate nonconforming  $hp$ /spectral element method to solve general elliptic boundary value problems with mixed Neumann and Dirichlet boundary conditions on non-smooth domains. In [18], a spectral element method for elliptic interface problems with smooth interfaces has been introduced and this has been extended to the elasticity interface problems in [15]. Blending elements have been used to completely resolve the interface and higher order approximation has been used.

In this article we propose a nonconforming spectral element method for elliptic interface problems with singularities based on [7, 16, 17]. A geometric mesh is used in the neighbourhood of the vertices and the auxiliary map of the form  $z = \ln \xi$  is introduced to remove the singularities at the corners, which was first introduced by Kondratiev in [19]. In the remaining part of the domain usual Cartesian coordinate system is used. The proposed method is essentially a least-squares method.

In the least-squares formulation of the method, a solution is sought which minimizes the sum of the squares of a weighted squared norms of the residuals in the partial differential equation and the sum of the squares of the residuals in the boundary conditions in fractional Sobolev norms and the sum of the squares of the jumps in the value and its normal derivatives of the function across the interface in appropriate fractional Sobolev norms and enforce the continuity along the inter element boundaries by adding a term which measures the sum of the squares of the jump in the function and its derivatives in fractional Sobolev norms.

The spectral element functions are nonconforming. The solution can be obtained by solving the normal equations using the preconditioned conjugate gradient method (PCGM) without computing the mass and stiffness matrices [16, 25]. An efficient preconditioner is used for the method which is a block diagonal matrix, where each diagonal block corresponds to an element [8]. The condition number of the preconditioner is  $O(\ln W)^2$ , where  $W$  is the degree of the approximating polynomial. Let  $N$  denote the number of layers in

the geometric mesh such that  $W$  is proportional to  $N$ . Then the method requires  $O(W \ln W)$  iterations of the PCGM to obtain the solution to exponential accuracy.

Here we define some Sobolev norms which are used in this article. Denote by  $H^m(\Omega)$  the Sobolev space of functions with square integrable derivatives of integer order  $\leq m$  on  $\Omega$  (a domain) furnished with the norm

$$\|u\|_{H^m(\Omega)}^2 = \sum_{|\alpha| \leq m} \|D^\alpha u\|_{L^2(\Omega)}^2.$$

Further, let

$$\|u\|_{s,I}^2 = \int_I u^2(x) dx + \int_I \int_I \frac{|u(x) - u(x')|^2}{|x - x'|^{1+2s}} dx dx'$$

denote the fractional Sobolev norm of order  $s$ , where  $0 < s < 1$ . Here  $I$  denotes an interval contained in  $\mathbb{R}$ .

For the definitions of the other function spaces which appears in this article, refer to [1, 9, 10]. Throughout the article we use  $x = (x_1, x_2)$  to represent a point on  $\mathbb{R}^2$  (in Cartesian coordinate system).

The contents of this paper are organized as follows: In Section 2 the elliptic interface problem is defined. Discretization of the domain and local transformation are described in Section 3. In Section 4, the numerical scheme has been derived. In Section 5 the computational results are provided for few test problems.

## 2 Interface Problem

In this section we state define the elliptic interface problem. For the convenience of the reader, we consider the polygonal domain as shown in the figure 1 for defining the interface problem, discretization and deriving the numerical scheme. The numerical method is also applicable for general polygonal domains with more number of vertices.

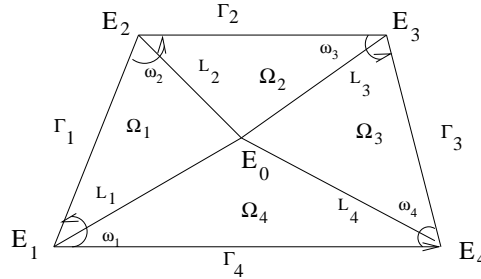


Figure 1: Polygonal domain with interfaces

Consider the polygonal domain  $\Omega$  in  $\mathbb{R}^2$  with boundary  $\partial\Omega = \Gamma$  as shown in the Fig. 1. Let  $E_i, i = 1, 2, 3, 4$  be the vertices of the domain. Let  $\Gamma = \cup_{i=1}^4 \Gamma_i$ , where  $\Gamma_i$  be the open edge of  $\partial\Omega$  connecting  $E_i$  and  $E_{i+1}$ . By  $\omega_i$  we denote the measure of the interior angle of  $\Omega$  at  $E_i$ . Without loss of generality, we will assume all interfaces meet at only one point  $E_0$  as shown in Fig. 1. Let  $(r, \theta) = (r_0, \theta_0)$  be the polar co-ordinates at the point  $E_0$  and suppose  $\Omega$  is decomposed into four subdomains  $\Omega_1, \Omega_2, \Omega_3, \Omega_4$  so that  $\overline{\Omega}_k \cap \overline{\Omega}_{k-1}$  is a straight line interface  $L_k, L_k = \{(r, \theta) : \theta = \Theta_k, 0 \leq r \leq R_k\}$ , for  $k = 1, 2, 3, 4$ .

### Elliptic Interface problem

Let us consider the following interface problem:

$$\begin{aligned} \mathcal{L}u &= -\nabla \cdot (p\nabla u) = f \text{ in } \cup \Omega_i \\ u &= 0 \text{ on } \Gamma_D = \cup_{i \in \mathcal{D}} \overline{\Gamma}_i \\ \frac{\partial u}{\partial n} &= g = G^N |_{\Gamma_N} \text{ on } \Gamma_N = \cup_{i \in \mathcal{N}} \overline{\Gamma}_i \end{aligned} \quad (1)$$

where  $\Gamma_D \cup \Gamma_N = \partial\Omega$ ,  $\mathcal{D} \cup \mathcal{N} = \{1, 2, \dots, 4\}$ ,  $\mathcal{D} \cap \mathcal{N} = \emptyset$ ,  $n = (n_1, n_2)$  is the unit normal vector on  $\Gamma_N$  and the coefficients are piecewise constants:

$$p = \begin{cases} p_1 & \text{in } \Omega_1 \\ p_2 & \text{in } \Omega_2 \\ \cdot & \cdot \\ p_4 & \text{in } \Omega_4 \end{cases}. \quad (2)$$

Assume that the interface conditions are satisfied. That is, on  $L_k$ ,  $1 \leq k \leq 4$ ,  $u$  satisfies

$$\begin{aligned} u(r, \Theta_k - 0) &= u(r, \Theta_k + 0) \\ p_{k-1} \frac{\partial u}{\partial n}(r, \Theta_k - 0) &= p_k \frac{\partial u}{\partial n}(r, \Theta_k + 0) \end{aligned} \quad (3)$$

where  $n = (n_1, n_2)$  is a unit normal vector to the interfaces  $L_k$ .

The asymptotic expansion, uniqueness and regularity of the solution of the above problem (1) - (3) has been discussed in detail in [10]. It has been shown that the solution has  $r^\lambda$  type of singularity near the points  $E_i$  which is similar to the singularity in the solution of elliptic problems on nonsmooth domains like domains with cracks and reentrant corners. But the strength of the singularity is strong in the elliptic interface problems.

### 3 Discretization and Stability

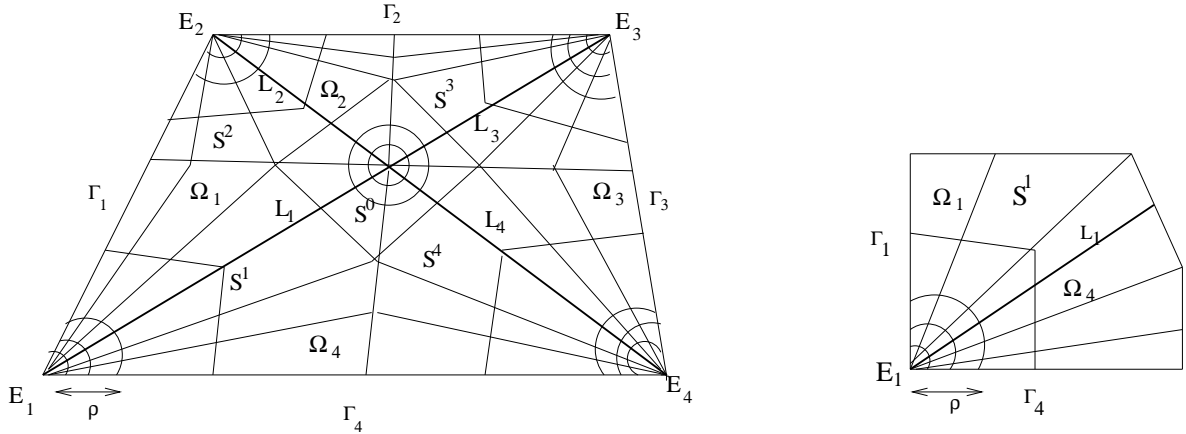


Figure 2: Discretization of the domain

Discretize the polygonal domain  $\Omega$  into 5 non-overlapping polygonal subdomains  $S^0, S^1, \dots, S^4$ . Here each  $S^k$  for  $k = 1, 2, 3, 4$  contains the vertex  $E_k$  only and contains a part of the interface  $L_k$  and  $S^0$  contains the point  $E_0$  and contains a part of all the interfaces  $L_k$  as shown in Fig. 2. Each subdomain  $S^k$ ,  $k \neq 0$  is a subset of union of two subdomains  $\Omega_i$  and  $\Omega_j$  for some  $i, j$ . For example  $S^1 \subset \Omega_1 \cup \Omega_4$  as shown in Fig. 2.

Let  $S^k = \left\{ \Omega_{i,j}^k : j = 1, 2, \dots, J_k, i = 1, 2, \dots, I_k \right\}$  be a partition of  $S^k$ ,  $k = 1, 2, 3, 4$  where  $J_k$  and  $I_k$  are integers. Let  $I_k$  be bounded and constant for all  $k = 1, 2, 3, 4$ . Let  $S^0 = \left\{ \Omega_{i,j}^0 : j = 1, 2, \dots, J_0, i = 1, 2, \dots, I_0 = 8 \right\}$  be a partition of  $S^0$  such that subdomain division matches on the interface. Let  $(r_k, \theta_k)$  denote polar coordinates with center at  $E_k$ .

Since the solution of the interface problem has singular behavior at  $E_i$ ,  $i = 1, 2, 3, 4$  where the interface intersects the boundary and also at  $E_0$  where the interfaces meet each other, we consider the geometric mesh and use the auxiliary mapping near each point  $E_i$ . The description of the geometric mesh and the auxiliary mapping is given below.

### Geometric mesh near $E_k, k \neq 0$

Let  $\{\psi_i^k\}_{i=1, \dots, I_k+1}$  be an increasing sequence of points such that  $\psi_1^k = \psi_l^k$  and  $\psi_{I_k+1}^k = \psi_u^k$ . Let  $\psi_i^k$  meet with interface for some  $i = I$ . That is,  $\psi_I^k$  matches with the interface  $L_k$  and hence separates  $\Omega_i$  and  $\Omega_j$  in  $S^k$ . Let  $\Delta\psi_i^k = \psi_{i+1}^k - \psi_i^k$ . Choose these points so that

$$\max_k \left( \max_i \Delta\psi_i^k \right) \leq \lambda \min_k \left( \min_i \Delta\psi_i^k \right)$$

for some constant  $\lambda$ .

Let  $\Pi^k = \{(x_1, x_2) : 0 < r_k < \rho\} \subseteq S^k$  be a sector with sides  $\Gamma_k$  and  $\Gamma_{k+1}$ . Now choose a geometric mesh with  $N$  layers in  $\Pi^k$  with a geometric ratio  $q_k$  ( $0 < q_k < 1$ ). Let  $\sigma_j^k = \rho (q_k)^{N+1-j}$  for  $2 \leq j \leq N+1$  and  $\sigma_1^k = 0$ .

Let

$$\Omega_{i,j}^k = \left\{ (x_1, x_2) : \sigma_j^k < r_k < \sigma_{j+1}^k, \psi_i^k < \theta_k < \psi_{i+1}^k \right\},$$

for  $1 \leq i \leq I_k, 1 \leq j \leq N$ .

Since  $S^k$  contains a part of the interface  $L_k$  and  $\psi_I^k$  meet with it, the elements  $\Omega_{I,j}^k$  and  $\Omega_{I-1,j}^k$  have the common edge which lies on the interface. For example, the elements  $\Omega_{I,j}^1 \subset \Omega_1$  and  $\Omega_{I-1,j}^1 \subset \Omega_4$  in  $S^1$  have the common edge on the interface  $L_1$ .

### Geometric mesh near $E_0$

Let  $\{\psi_i^0\}_{i=1, \dots, 9}$  be an increasing sequence of points such that  $\psi_1^0 = 0$  and  $\psi_9^0 = 2\pi$  and  $\psi_i^0$  for some  $i$  meet with interfaces  $L_k$ .

Let  $\Pi^0 = \{(x_1, x_2) : 0 < r_0 < \rho\} \subseteq S^0$  be a circular region around  $E_0$ . Now choose a geometric mesh with  $N$  layers in  $\Pi^0$  with a geometric ratio  $q_0$  ( $0 < q_0 < 1$ ). Let  $\sigma_j^0 = \rho (q_0)^{N+1-j}$  for  $2 \leq j \leq N+1$  and  $\sigma_1^0 = 0$ .

Let

$$\Omega_{i,j}^0 = \left\{ (x_1, x_2) : \sigma_j^0 < r_0 < \sigma_{j+1}^0, \psi_i^0 < \theta_0 < \psi_{i+1}^0 \right\},$$

for  $1 \leq i \leq 8, 1 \leq j \leq N$ .

### In the remaining part of $S^k$

In the remaining part of  $S^k, 1 \leq k \leq 4$ , we retain the Cartesian coordinate system  $(x_1, x_2)$  i.e., in  $\Omega_{i,j}^k$  for  $1 \leq i \leq I_k, N < j \leq J_k$ .

Let

$$\Omega^1 = \left\{ \Omega_{i,j}^k : 1 \leq i \leq I_k, N < j \leq J_k, 1 \leq k \leq 4 \right\}.$$

Similarly we retain the Cartesian coordinate system  $(x_1, x_2)$  in the remaining part of  $S^0$ .

Let

$$\Omega^0 = \left\{ \Omega_{i,j}^0 : 1 \leq i \leq 8, N < j \leq J_k \right\}.$$

Here for  $i = 1, 8, \Omega_{i,j}^0 \subseteq \Omega_3$ ;  $i = 2, 3, \Omega_{i,j}^0 \subseteq \Omega_2$ ;  $i = 4, 5, \Omega_{i,j}^0 \subseteq \Omega_1$ ;  $i = 6, 7, \Omega_{i,j}^0 \subseteq \Omega_4$ . For  $j > N$ ,  $\Omega_{1,j}^0$  and  $\Omega_{2,j}^0$  have a common edge which lies on  $L_3$ . Similarly, the elements  $\Omega_{1,j}^0$  &  $\Omega_{2,j}^0$ ,  $\Omega_{3,j}^0$  &  $\Omega_{4,j}^0$ ,  $\Omega_{5,j}^0$  &  $\Omega_{6,j}^0$  and  $\Omega_{7,j}^0$  &  $\Omega_{8,j}^0$  have the common edges which lies on  $L_3, L_2, L_1$  and  $L_4$  respectively.

### Auxiliary Mapping

Now let  $\tau_k = \ln r_k$  in  $\{(x_1, x_2) : 0 < r_k < \rho\} \subseteq S^k$ ,  $0 \leq k \leq 4$ . Define  $\zeta_j^k = \ln \sigma_j^k$  for  $1 \leq j \leq N+1$ . Here  $\zeta_1^k = -\infty$ . Define

$$\tilde{\Omega}_{i,j}^k = \left\{ (\tau_k, \theta_k) : \zeta_j^k < \tau_k < \zeta_{j+1}^k, \psi_i^k < \theta_k < \psi_{i+1}^k \right\},$$

for  $1 \leq i \leq I_k, 1 \leq j \leq N$ . Hence the geometric mesh  $\Omega_{i,j}^k$ ,  $2 \leq j \leq N$  becomes a quasi-uniform mesh in modified polar coordinates (Fig. 3). However,  $\tilde{\Omega}_{i,1}^k$  is a semi-infinite strip.

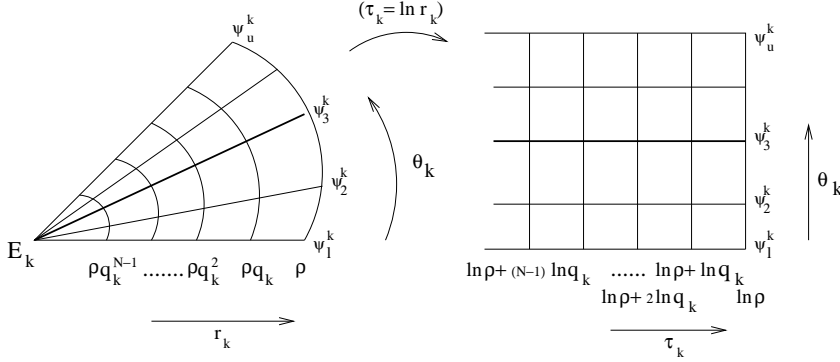


Figure 3: Quasi uniform mesh in  $\tau_k$  and  $\theta_k$  coordinates near  $E_k, k \neq 0$ .

### Approximation

The nonconforming spectral element functions are sum of tensor products of polynomials of degree  $W_j$ ,  $1 \leq W_j \leq W$  in their respective modified polar coordinates (4) in  $\tilde{\Omega}_{i,j}^k$  for  $0 \leq k \leq 4, 1 \leq i \leq I_k, 2 \leq j \leq N$ . In the infinite sector i.e., in  $\tilde{\Omega}_{i,1}^k$ , the solution is approximated by a constant which is the value of the function  $u$  at the corresponding point  $E_k$ . The constant value is computed by treating it as a common boundary value during the numerical computation.

Let  $u_{i,1}^k(\tau_k, \theta_k) = h_k$ , a constant on  $\tilde{\Omega}_{i,1}^k$ . Define the spectral element function

$$u_{i,j}^k(\tau_k, \theta_k) = \sum_{r=0}^{W_j} \sum_{s=0}^{W_j} g_{r,s} \tau_k^r \theta_k^s, \quad (4)$$

on  $\tilde{\Omega}_{i,j}^k$  for  $1 \leq i \leq I_k, 2 \leq j \leq N, 0 \leq k \leq 4$ . Here  $1 \leq W_j \leq W$ .

Moreover there is an analytic mapping  $M_{i,j}^k$  from the master square  $S = (-1, 1)^2$  to the elements  $\Omega_{i,j}^k$  in  $\Omega^0$  and  $\Omega^1$ . Define

$$u_{i,j}^k(M_{i,j}^k(\xi, \eta)) = \sum_{r=0}^W \sum_{s=0}^W g_{r,s} \xi^r \eta^s. \quad (5)$$

## 4 Numerical Scheme

Here we describe the numerical formulation. This numerical method is essentially a least-squares formulation based on [16, 18].

As defined in Section 3,  $\tilde{\Omega}_{i,j}^k$  is the image of  $\Omega_{i,j}^k$  in  $(\tau_k, \theta_k)$  coordinates. Let  $\mathcal{L}_{i,j}^k$  be the operator defined by  $\mathcal{L}_{i,j}^k u = r_k^2 \mathcal{L} u$ . Then the operator  $\tilde{\mathcal{L}}_{i,j}^k$  in the transformed coordinates  $\tau_k$  and  $\theta_k$  is given by

$$\tilde{\mathcal{L}}_{i,j}^k u = -p \left( \frac{\partial^2 u}{\partial \tau_k^2} + \frac{\partial^2 u}{\partial \theta_k^2} \right).$$

Where  $p$  takes different values based on  $i$  value as explained in Section 3.

Next, let the vertex  $E_k = (x_1^k, x_2^k)$  and

$$F_{i,j}^k(\tau_k, \theta_k) = e^{2\tau_k} f\left(x_1^k + e^{\tau_k} \cos \theta_k, x_2^k + e^{\tau_k} \sin \theta_k\right)$$

in  $\tilde{\Omega}_{i,j}^k$  for  $0 \leq k \leq 4$ ,  $2 \leq j \leq N$ ,  $1 \leq i \leq I_k$ .

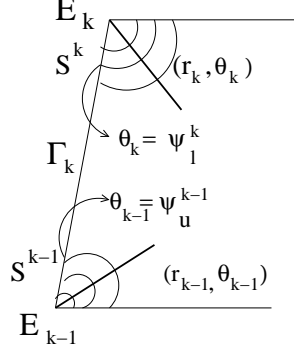


Figure 4: Edge  $\Gamma_k$  common to  $\Pi^{k-1}$  and  $\Pi^k$

Consider the boundary  $\frac{\partial u}{\partial n} = g$  on  $\Gamma_k \cap \partial \Pi^k$  for  $k \in \mathcal{N}$  (see Fig. 4). Let

$$l_1^k(\tau_k) = \frac{\partial u^k}{\partial n} = e^{\tau_k} g(x_1^k + e^{\tau_k} \cos(\psi_1^k), x_2^k + e^{\tau_k} \sin(\psi_1^k)).$$

Consider  $\frac{\partial u}{\partial n} = g$  for  $k \in \mathcal{N}$  on  $\Gamma_k \cap \partial \Pi^{k-1}$  (look at Fig. 4). Define

$$l_2^k(\tau_{k-1}) = \frac{\partial u^k}{\partial n} = e^{\tau_{k-1}} g(x_1^{k-1} + e^{\tau_{k-1}} \cos(\psi_u^{k-1}), x_2^{k-1} + e^{\tau_{k-1}} \sin(\psi_u^{k-1})).$$

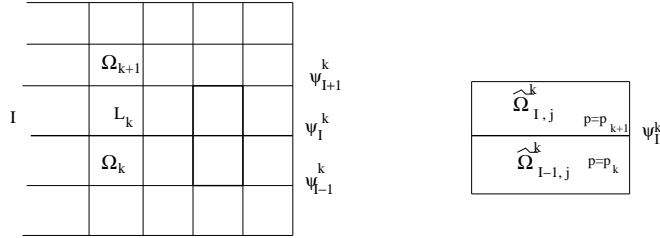


Figure 5: Elements with interface as common edge

As described in section 3,  $\psi_I^k$  matches with the interface  $L_k$ , the elements  $\Omega_{I,j}^k$  and  $\Omega_{I-1,j}^k$  have the common edge  $\gamma_s$ . Let  $\tilde{\gamma}_s$  be the image of  $\gamma_s$  in  $\tau_k$  and  $\theta_k$  coordinates and therefore  $\tilde{\gamma}_s$  is the common edge of  $\tilde{\Omega}_{I,j}^k$  and  $\tilde{\Omega}_{I-1,j}^k$  which lies on  $L_k$ . We define the jump in the solution across  $\gamma_s \subseteq L_k$

$$\| [u^k] \|_{\frac{3}{2}, \tilde{\gamma}_s}^2 = \| u_{I,j}^k(\tau_k, \psi_I^k) - u_{I-1,j}^k(\tau_k, \psi_I^k) \|_{0, \tilde{\gamma}_s}^2 + \left\| \frac{\partial u_{I,j}^k}{\partial \tau_k}(\tau_k, \psi_I^k) - \frac{\partial u_{I-1,j}^k}{\partial \tau_k}(\tau_k, \psi_I^k) \right\|_{\frac{1}{2}, \tilde{\gamma}_s}^2.$$

Now we define the jump across the normal derivative across the interface

$$\left\| \left[ p \frac{\partial u^k}{\partial \theta_k} \right] \right\|_{\frac{1}{2}, \tilde{\gamma}_s}^2 = \left\| p_{k+1} \frac{\partial u_{I,j}^k}{\partial \theta_k}(\tau_k, \psi_I^k) - p_k \frac{\partial u_{I-1,j}^k}{\partial \theta_k}(\tau_k, \psi_I^k) \right\|_{\frac{1}{2}, \tilde{\gamma}_s}^2.$$

In similar way, we define the term which measures the sum of the squares of the jump in  $u$  and its derivatives with respect to  $\tau_k$  and  $\theta_k$  in appropriate Sobolev norms along the inter-element boundaries.

In the remaining part of the domain, i.e on  $\Omega^1$  and  $\Omega^0$  the solution is smooth. The residue in the equation and jumps across the interfaces and inter element boundaries and residue at the boundary has been described in detail in [18]. Here we define the functional near the singularities and in the interior.

Let  $\gamma_s \subseteq \bar{\Pi}^k$  and  $d(E_k, \gamma_s) = \inf_{x \in \gamma_s} \{\text{distance}(E_k, x)\}$ . Choose  $\alpha_k = 1 - \beta_k$  as defined in [7]. Let  $\mathcal{F}_u = \left\{ \left\{ u_{i,j}^k(\tau_k, \theta_k) \right\}_{i,j,k}, \left\{ u_{i,j}^k(\xi, \eta) \right\}_{i,j,k} \right\} \in \Pi^{N,W}$ , the space of spectral element functions. Define  $a_k = u(E_k)$ . Define the functional

$$\begin{aligned}
\mathfrak{r}_{\text{vertices}}^{N,W}(\mathcal{F}_u) &= \sum_{k=0}^4 \sum_{j=2}^N \sum_{i=1}^{I_k} (\rho \mu_k^{N+1-j})^{-2\alpha_k} \left\| (\mathcal{L}_{i,j}^k) u_{i,j}^k(\tau_k, \theta_k) - F_{i,j}^k(\tau_k, \theta_k) \right\|_{0, \bar{\Omega}_{i,j}^k}^2 \\
&+ \sum_{k=0}^4 \sum_{\substack{\gamma_s \subseteq \Pi^k, \gamma_s \not\subseteq L_k \\ \mu(\tilde{\gamma}_s) < \infty}} d(E_k, \gamma_s)^{-2\alpha_k} \left( \| [u^k] \|_{0, \tilde{\gamma}_s}^2 + \| [(u_{\tau_k}^k)] \|_{1/2, \tilde{\gamma}_s}^2 + \| [(u_{\theta_k}^k)] \|_{1/2, \tilde{\gamma}_s}^2 \right) \\
&+ \sum_{k=0}^4 \sum_{\gamma_s \subseteq L_k} d(E_k, \gamma_s)^{-2\alpha_k} \left( \| [u^k] \|_{\frac{3}{2}, \tilde{\gamma}_s}^2 + \left\| \left[ p \frac{\partial u^k}{\partial \theta_k} \right] \right\|_{\frac{1}{2}, \tilde{\gamma}_s}^2 \right) \\
&+ \sum_{m \in \mathcal{D}} \sum_{k=m-1}^m \sum_{\substack{\gamma_s \subseteq \partial \Pi^k \cap \Gamma_m \\ \mu(\tilde{\gamma}_s) < \infty}} d(E_k, \gamma_s)^{-2\alpha_k} \left( \| (u^k - h_k) - (l_{m-k+1}^m - a_k) \|_{0, \tilde{\gamma}_s}^2 \right. \\
&+ \left. \| u_{\tau_k}^k - (l_{m-k+1}^m)_{\tau_k} \|_{1/2, \tilde{\gamma}_s}^2 \right) + \sum_{m \in \mathcal{D}} \sum_{k=m-1}^m (h_k - a_k)^2 \\
&+ \sum_{m \in \mathcal{N}} \sum_{k=m-1}^m \sum_{\substack{\gamma_s \subseteq \partial \Pi^k \cap \Gamma_m \\ \mu(\tilde{\gamma}_s) < \infty}} d(E_k, \gamma_s)^{-2\alpha_k} \left\| \left( \frac{\partial u^k}{\partial n} \right) - l_{m-k+1}^m \right\|_{1/2, \tilde{\gamma}_s}^2.
\end{aligned} \tag{6}$$

In the above  $\mu(\tilde{\gamma}_s)$  denotes the measure of  $\tilde{\gamma}_s$ .

Define

$$\begin{aligned}
\mathfrak{r}_{\text{interior}}^{N,W}(\mathcal{F}_u) &= \sum_{k=0}^4 \sum_{j=N+1}^{J_k} \sum_{i=1}^{I_k} \left\| (\mathcal{L}_{i,j}^k) u_{i,j}^k(\xi, \eta) - F_{i,j}^k(\xi, \eta) \right\|_{0, \Omega_{i,j}^k}^2 \\
&+ \sum_{\gamma_s \subseteq \Omega^0 \cup \Omega^1, \gamma_s \not\subseteq L_k} \left( \| [u^k] \|_{0, \gamma_s}^2 + \| [(u_{x_1}^k)] \|_{1/2, \gamma_s}^2 + \| [(u_{x_2}^k)] \|_{1/2, \gamma_s}^2 \right) \\
&+ \sum_{\gamma_s \subseteq L_k \subseteq \Omega^0 \cup \Omega^1} \left( \| [u^k] \|_{\frac{3}{2}, \gamma_s}^2 + \left\| \left[ \left( p \frac{\partial u^k}{\partial n} \right) \right] \right\|_{1/2, \gamma_s}^2 \right) \\
&+ \sum_{l \in \mathcal{D}} \sum_{\gamma_s \subseteq \partial \Omega^1 \cap \Gamma_l} \left( \| (u^k - o^{l,k}) \|_{0, \gamma_s}^2 + \left\| \left( \frac{\partial u^k}{\partial T} \right) - \left( \frac{\partial o^{l,k}}{\partial T} \right) \right\|_{1/2, \gamma_s}^2 \right) \\
&+ \sum_{l \in \mathcal{N}} \sum_{\gamma_s \subseteq \partial \Omega^1 \cap \Gamma_l} \left\| \left( \frac{\partial u^k}{\partial n} \right) - o^{l,k} \right\|_{1/2, \gamma_s}^2.
\end{aligned} \tag{7}$$

Let

$$\mathfrak{r}^{N,W}(\mathcal{F}_u) = \mathfrak{r}_{\text{vertices}}^{N,W}(\mathcal{F}_u) + \mathfrak{r}_{\text{interior}}^{N,W}(\mathcal{F}_u).$$

We choose as our approximate solution the unique  $\mathcal{F}_z \in \Pi^{N,W}$ , the space of spectral element functions, which minimizes the functional  $\mathfrak{r}^{N,W}(\mathcal{F}_u)$  over all  $\mathcal{F}_u$ .

The method is essentially a least-squares method and the solution is obtained at Gauss-Legendre-Lobatto points using preconditioned conjugate gradient method without storing the stiffness matrix and load vector. The residuals in the normal equations can be computed efficiently and inexpensively as shown in [17, 25].

The minimization leads to the normal equations

$$AU = h.$$



The vector  $U$  composed of the values of the spectral element functions at Gauss-Legendre-Lobatto points is divided into two sub vectors one consisting of the values of the spectral element functions at the vertices of the domain constitute the set of common boundary values  $U_B$ , and the other consisting of the remaining values which we denote by  $U_I$ . The computation of  $U_I$  and  $U_B$  is described in [17, 25].

An efficient preconditioner has been used which is proposed in [8] for the matrix  $A$  so that the condition number of the preconditioned system is as small as possible. The condition number of the preconditioned system is  $O((\ln W)^2)$ . The preconditioner is a block diagonal matrix, where each diagonal block is constructed using the separation of variable technique. So the solution is obtained to an exponential accuracy using  $O(W \ln W)$  iterations of the PCGM. After obtaining the nonconforming solution at the Gauss-Legendre-Lobatto points, a set of corrections are performed [26] so that the solution is conforming and belongs to  $H^1(\Omega)$ .

Then for  $W$  large enough the error estimate

$$\|u - u_{ap}\|_{1,\Omega} \leq C e^{-bW}$$

holds, where  $C$  and  $b$  are constants and  $u_{ap}$  is the corrected solution.

## 5 Numerical Results

Here we consider few numerical examples to show the effectiveness of the proposed method. For simplicity, we have considered  $W_j = W$  for all  $j$  and the number of layers  $N = W$  in the geometric mesh. The relative error  $\|e\|_{ER} = \frac{\|e\|_1}{\|u\|_1}$ , where  $e = u - u_{ap}$  is the difference in the exact solution  $u$  and the approximate solution  $u_{ap}$  measured in  $H^1$  norm. ‘‘Iters’’ is the total number of iterations to compute  $U_I$  and  $U_B$ .

### Example 1: Interface problem with singularity at the intersection of an interface and the boundary

Let us consider the interface problem on the domain  $\Omega = \Omega_1 \cup \Omega_2$  as shown in Fig. 6

$$\begin{aligned} -\nabla \cdot (p \nabla u) &= 0 \text{ in } \Omega \\ u &= 0 \text{ on } \Gamma_1 \\ \frac{\partial u}{\partial \theta} &= 0 \text{ on } \Gamma_2 \end{aligned}$$

where the coefficient  $p$  is piecewise constant:

$$p = \begin{cases} 1 & \text{in } \Omega_1 \\ p & \text{in } \Omega_2. \end{cases}$$

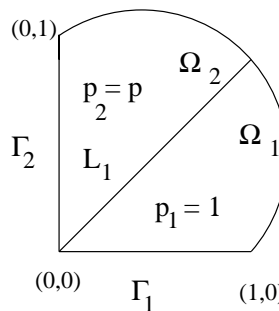


Figure 6: The interface problem on a sector

Let  $(r, \theta)$  be the polar coordinates centered at the origin  $(0, 0)$ . Assume that the interface conditions are

satisfied at  $\theta = \frac{\pi}{4}$ . That is, on  $L_1$

$$\begin{aligned} u(r, \frac{\pi}{4} - 0) &= u(r, \frac{\pi}{4} + 0) \\ \frac{\partial u}{\partial \theta}(r, \frac{\pi}{4} - 0) &= p \frac{\partial u}{\partial \theta}(r, \frac{\pi}{4} + 0). \end{aligned}$$

Let the solution of the above interface problem be in the form  $r^\lambda W(\theta)$ . As explained in [10, 24],  $\lambda$  and  $W(\theta)$  can be obtained by solving the following Sturm-Liouville problem corresponding to the above interface problem:

$$\begin{aligned} \frac{d}{d\theta}(p \frac{dW}{d\theta}) + \lambda^2 p W &= 0 \text{ in } \Omega \\ W(0) = 0, \frac{dW}{d\theta}(\frac{\pi}{2}) &= 0. \end{aligned} \quad (8)$$

The function  $W(\theta)$  required to satisfy

$$\begin{aligned} W(\frac{\pi}{4} - 0) &= W(\frac{\pi}{4} + 0) \\ \frac{dW}{d\theta}(\frac{\pi}{4} - 0) &= p \frac{dW}{d\theta}(\frac{\pi}{4} + 0). \end{aligned} \quad (9)$$

The solution of the above differential equation  $W$  is of the form

$$W(\theta) = \begin{cases} C_1 \cos \lambda \theta + C_2 \sin \lambda \theta & \text{in } \Omega_1 \\ C_3 \cos \lambda \theta + C_4 \sin \lambda \theta & \text{in } \Omega_2 \end{cases}$$

Therefore the solution of the interface problem has the following form

$$\begin{aligned} u_1 &= r^\lambda (C_1 \cos \lambda \theta + C_2 \sin \lambda \theta) \text{ in } \Omega_1 \\ u_2 &= r^\lambda (C_3 \cos \lambda \theta + C_4 \sin \lambda \theta) \text{ in } \Omega_2. \end{aligned}$$

The constants  $C_1, C_2, C_3$  and  $C_4$  and the eigenvalues  $\lambda$  can be obtained using the above defined boundary and interface conditions (8) and (9).

Now, after applying the boundary conditions, we get

$$\begin{aligned} W(0) = 0 &\rightarrow C_1 = 0 \\ \frac{dW}{d\theta}(\frac{\pi}{2}) = 0 &\rightarrow -C_3 \sin \frac{\lambda \pi}{2} + C_4 \cos \frac{\lambda \pi}{2} = 0. \end{aligned}$$

The interface conditions gives

$$\begin{aligned} W(\frac{\pi}{4} -) &= W(\frac{\pi}{4} +) \\ \Rightarrow C_2 \sin \frac{\lambda \pi}{4} - C_3 \cos \frac{\lambda \pi}{4} - C_4 \sin \frac{\lambda \pi}{4} &= 0 \end{aligned}$$

and

$$\begin{aligned} \frac{dW}{d\theta}(\frac{\pi}{4} - 0) &= p \frac{dW}{d\theta}(\frac{\pi}{4} + 0) \\ \Rightarrow C_2 \cos \frac{\lambda \pi}{4} + C_3 p \sin \frac{\lambda \pi}{4} - C_4 p \cos \frac{\lambda \pi}{4} &= 0. \end{aligned}$$

So we have the following homogeneous system

$$\begin{bmatrix} 0 & -\sin \frac{\lambda \pi}{2} & \cos \frac{\lambda \pi}{2} \\ \sin \frac{\lambda \pi}{4} & -\cos \frac{\lambda \pi}{4} & -\sin \frac{\lambda \pi}{4} \\ \cos \frac{\lambda \pi}{4} & p \sin \frac{\lambda \pi}{4} & -p \cos \frac{\lambda \pi}{4} \end{bmatrix} \begin{bmatrix} C_2 \\ C_3 \\ C_4 \end{bmatrix} = \begin{bmatrix} 0 \\ 0 \\ 0 \end{bmatrix}. \quad (10)$$

In order for the system of unknowns  $C_2, C_3, C_4$  to have a non-trivial solution, the determinant of the coefficient matrix  $A$  of the system should be zero.

$$\begin{aligned} & \begin{vmatrix} 0 & -\sin\frac{\lambda\pi}{2} & \cos\frac{\lambda\pi}{2} \\ \sin\frac{\lambda\pi}{4} & -\cos\frac{\lambda\pi}{4} & -\sin\frac{\lambda\pi}{4} \\ \cos\frac{\lambda\pi}{4} & p\sin\frac{\lambda\pi}{4} & -p\cos\frac{\lambda\pi}{4} \end{vmatrix} = 0 \\ \implies & \frac{(1-p)}{2}\sin^2\frac{\lambda\pi}{2} + \cos\frac{\lambda\pi}{2} + (p-1)\sin^2\frac{\lambda\pi}{4}\cos\frac{\lambda\pi}{2} = 0 \\ \implies & \frac{(1-p)}{2}\sin^2\frac{\lambda\pi}{2} + \cos\frac{\lambda\pi}{2} + \frac{(p-1)}{2}(1-\cos\frac{\lambda\pi}{2})\cos\frac{\lambda\pi}{2} = 0 \\ \implies & \frac{(1-p)}{2} + \left[\frac{(p-1)}{2} + 1\right]\cos\frac{\lambda\pi}{2} = 0. \end{aligned}$$

By solving  $\frac{(1-p)}{2} + \left[\frac{(p-1)}{2} + 1\right]\cos\frac{\lambda\pi}{2} = 0$ , we obtain the eigenvalues  $\lambda_k$  which are positive real values. The smallest eigenvalue  $\lambda_0$  among  $\lambda_k$  gives the value of the exponent in the leading order singular term in the expansion of  $u$ . The value of  $\lambda_0$  for different values of  $p$  is given in the following Table 1. The strength of the singularity increases as  $p$  increases.

$p$	$\lambda_0$
5	0.53544092
10	0.38996444
30	0.22992823
50	0.1788770
100	0.12690206

Table 1: The exponent of leading order singular term for different  $p$

Now, we find the constants  $C_2, C_3$  and  $C_4$ . From the above linear system

$$C_4 = C_3 \frac{\sin\frac{\lambda\pi}{2}}{\cos\frac{\lambda\pi}{2}} = C_3 \tan\frac{\lambda\pi}{2}.$$

We choose  $C_3 = 1$ . Therefore  $C_4 = \tan\frac{\lambda\pi}{2}$ . Then, one can easily find the value of  $C_2$  from any one of the equations in the linear system. The value of  $C_2$  is given by

$$C_2 = \cot\frac{\lambda\pi}{4} + \tan\frac{\lambda\pi}{2}.$$

Therefore the leading order singular term in the expansion of  $u$  has the following form

$$\begin{aligned} u_1 &= r^{\lambda_0} \left( \cot\frac{\lambda_0\pi}{4} + \tan\frac{\lambda_0\pi}{2} \right) \sin\lambda_0\theta \text{ in } \Omega_1 \\ u_2 &= r^{\lambda_0} \left( \cos\lambda_0\theta + \tan\frac{\lambda_0\pi}{2} \sin\lambda_0\theta \right) \text{ in } \Omega_2. \end{aligned}$$

**Remark:** The solution  $u$  has singular behavior at the point  $(0,0)$  and the strength of the singularity is very strong for larger values of  $p$ . These singularities are more stronger than the singularities which generally arises in elliptic problems due to the nonsmooth domains.

Now we present the numerical solution of this problem. We consider the Dirichlet boundary condition on  $\rho = 1$  ( Fig. 6). Since the strength of the singularity is very strong at the corners a very refined mesh as well as higher degree of approximation is needed to get a good accuracy. In [10] the numerical solution is obtained using  $hp$  finite element method. They have used a geometric mesh near the corner with geometric ratio 0.15 and tabulated the relative error for different values of the degree of approximation  $W$  with  $2W$  layers in the geometric mesh in the radial direction.

In the following table we have presented the numerical results for  $p = 5$ . As explained above the exponent in the leading order singular term in the solution for  $p = 5$  is 0.53544092. We consider the geometric ratio  $\mu = 0.15$ . The relative error is obtained for different values of  $W$  and shown in the following Table 2. Table 2 also shows the number of iterations.

$W$	$\ e\ _{ER} \%$	Iters
2	11.254417	37
3	4.29850	77
4	1.541124	118
5	0.5575801	159
6	0.2017785	204
7	0.0730631	250
8	0.0264555	291
9	0.0095797	335

Table 2: The relative error and iterations against  $W$

Fig. 7 shows the log of the relative error against the degree of approximation  $W$  and the relation is linear. This shows the exponential accuracy of the method.

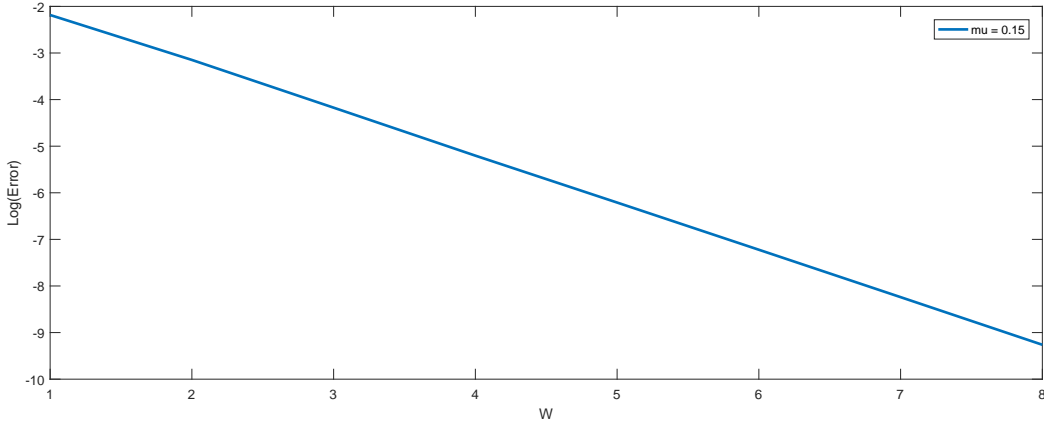


Figure 7: Log of  $\|e\|_{ER}$  against  $W$

Now we consider  $p = 10$ . The exponent in the leading order singular term of the solution is 0.38996444. This is strong compared to the previous exponent. So we need more refined grid near the singular point. Here we consider the geometric ratio  $\mu = 0.15$  and  $\mu = e^{-\pi}$ . The relative error and iteration count for different values of  $W$  is tabulated in the Table 3.

$W$	$\mu = 0.15$		$\mu = e^{-\pi}$	
	$\ e\ _{ER} \%$	Iters	$\ e\ _{ER} \%$	Iters
2	19.08735	44	7.19601	48
3	9.632562	95	2.300786	122
4	4.66738	159	0.676060	208
5	2.24022	226	0.198810	279
6	1.07102	290	0.058287	368
7	0.511375	346	0.017128	449
8	0.244061	424	0.00503136	525
9	0.116472	474	0.00147676	623

Table 3: The relative error and iterations against  $W$  for  $\mu = 0.15$  and  $\mu = e^{-\pi}$

The error decays slowly for the geometric ratio  $\mu = 0.15$ . One can get better accuracy by increasing the

number of layers in the geometric mesh. But this increases the number of degrees of freedom. For  $\mu = e^{-\pi}$  the error decays very fast with an increase in the iteration count. Even better accuracy can be achieved with the geometric ratio  $\mu = e^{-1.5\pi}$ . In the Figure 8 the graph of log of relative error vs.  $W$  has been drawn for  $\mu = 0.15$  and  $\mu = e^{-\pi}$ . The relation is linear.

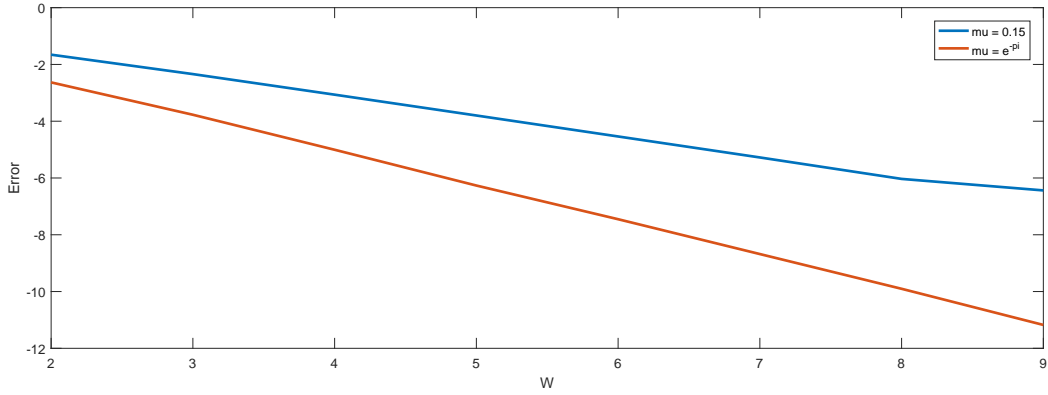


Figure 8: Log of  $\|e\|_{ER}$  against  $W$

Now we consider  $p = 30$ . In this case the exponent in the leading order singular term of the solution is 0.22992823. Here we consider four different geometric mesh with ratio  $\mu = 0.15, \mu = 0.15$  with more number of layers (just double of the degree of the approximation  $W$ ) in radial direction,  $\mu = e^{-\pi}$  and  $\mu = e^{-1.5\pi}$ . The relative error and iterations are shown for different values of  $W$  and for different geometric ratios in Table 4.

$W$	$\mu = 0.15$		$\mu = 0.15$		$\mu = e^{-\pi}$		$\mu = e^{-1.5\pi}$	
	$\ e\ _{ER} \%$	Iters	$\ e\ _{ER} \%$	Iters	$\ e\ _{ER} \%$	Iters	$\ e\ _{ER} \%$	Iters
2	32.48562	49	14.36468	103	18.848278	60	9.12371	63
3	22.58167	122	6.68331	244	10.28457	156	3.53691	169
4	15.27828	212	2.83311	402	5.123292	272	1.210048	326
5	10.16691	308	1.118838	551	2.50895	404	0.409445	500
6	6.68372	409	0.496950	721	1.22152	548	0.138267	713
7	4.36046	502	0.207736	891	0.593652	667	0.046691	898
8							0.015766	1051
9							0.005324	1263

Table 4: The relative error and iterations against  $W$

The results shows the geometric ratio  $\mu = e^{-1.5\pi}$  gives better results. Even better accuracy can be achieved with the geometric ratio  $\mu = e^{-2\pi}$  with an increase in the number of iterations. The Fig. 9 shows the graph of log of relative error against  $W$  for different values of  $\mu$ . The relation is linear in all cases but the convergence is faster for  $\mu = e^{-1.5\pi}$ .

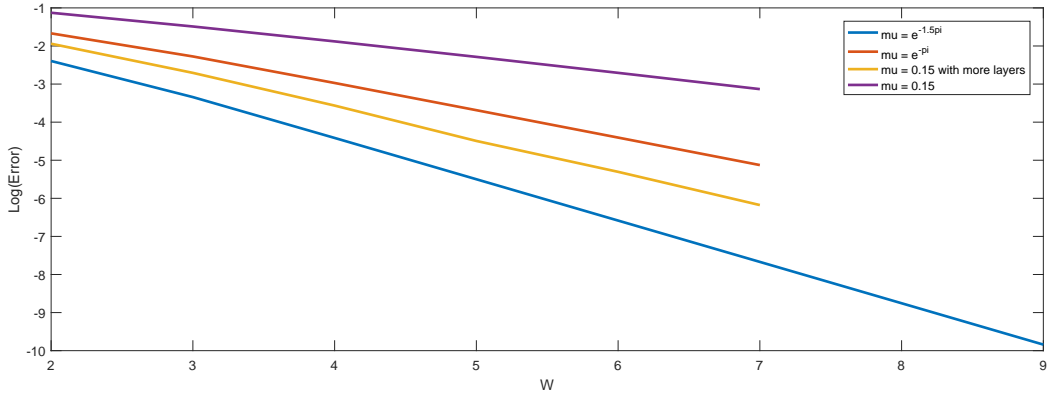


Figure 9: Log of  $\|e\|_{ER}$  against  $W$

Now consider  $p = 50, 100$ . The exponents in the leading order singular term of the solution are 0.1788770 and 0.12690206 respectively. So we need very refined mesh in the neighbourhood of the singular point. So we consider the geometric ratio  $\mu = e^{-2\pi}$ . The relative error and iterations are tabulated for different values of  $W$  in Table 5. The numerical results shows the good performance of the method.

$p = 50$			$p = 100$	
$W$	$\ e\ _{ER} \%$	Iters	$\ e\ _{ER} \%$	Iters
2	8.353101	80	15.9732	92
3	3.119198	219	8.29721	241
4	1.019195	438	3.83097	475
5	0.330973	700	1.73125	778
6	0.106907	1030	0.777691	1137
7	0.034519	1354	0.348880	1486
8	0.011145	1631	0.156460	1806
9	0.003598	1967	0.0701626	2358

Table 5: The relative error and iterations against  $W$

Fig. 10 shows the graph of log relative error against  $W$  for  $p = 50$  and  $p = 100$ . The relation is linear. This show the exponential convergence of the proposed method.

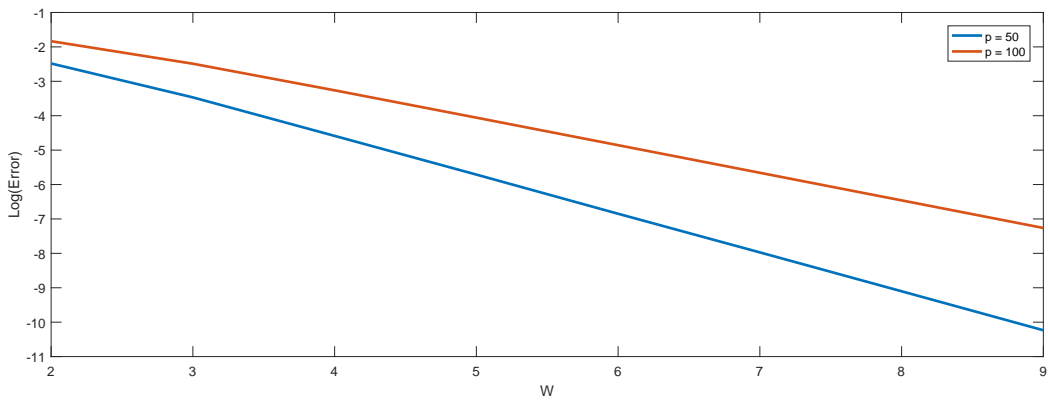


Figure 10: Log of  $\|e\|_{ER}$  against  $W$

### Example 2: Interface problem with singularity at the intersection of two interfaces

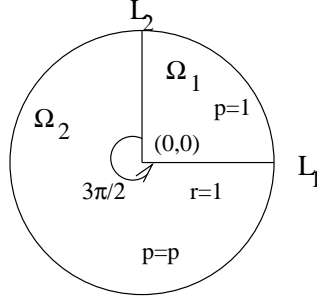


Figure 11: The domain  $\Omega$  with  $L_1$  and  $L_2$  meet at  $(0,0)$

Consider the following interface problem on the domain  $\Omega$  as shown in Fig. 11.

$$-\nabla \cdot (p \nabla u) = 0 \text{ in } \Omega$$

where the coefficient  $p$  is piecewise constant:

$$p = \begin{cases} 1 & \text{in } \Omega_1 \\ p & \text{in } \Omega_2 \end{cases}$$

with Dirichlet boundary condition on the circle of radius 1. Assume that the two interfaces  $L_1 = \{(r,0), 0 \leq r \leq 1\}$  and  $L_2 = \{(r, \frac{\pi}{2}), 0 \leq r \leq 1\}$  meets at the point  $E_0 = (0,0)$  and  $u$  satisfies the interface conditions

$$\begin{aligned} u(\theta = 0) &= u(\theta = 2\pi) \text{ and } \frac{\partial u}{\partial \theta}(0) = p \frac{\partial u}{\partial \theta}(2\pi) \\ u(\frac{\pi}{2}-) &= u(\frac{\pi}{2}+) \text{ and } \frac{\partial u}{\partial \theta}(\frac{\pi}{2}-) = p \frac{\partial u}{\partial \theta}(\frac{\pi}{2}+). \end{aligned}$$

Here we are only interested in the behavior of the solution at  $(0,0)$ . So as explained in Section 2, we need to solve the Sturm-Liouville problem

$$\frac{d}{d\theta} (p \frac{dW}{d\theta}) + \lambda^2 p W = 0 \text{ in } \Omega$$

with

$$\begin{aligned} W(\theta = 0) &= W(\theta = 2\pi) \text{ and } \frac{dW}{d\theta}(0) = p \frac{dW}{d\theta}(2\pi) \\ W(\frac{\pi}{2}-) &= W(\frac{\pi}{2}+) \text{ and } \frac{dW}{d\theta}(\frac{\pi}{2}-) = p \frac{dW}{d\theta}(\frac{\pi}{2}+). \end{aligned}$$

The solution of the above differential equation  $W$  is of the form

$$W(\theta) = \begin{cases} C_1 \cos \lambda \theta + C_2 \sin \lambda \theta & \text{in } \Omega_1 \\ C_3 \cos \lambda \theta + C_4 \sin \lambda \theta & \text{in } \Omega_2. \end{cases}$$

As explained in the above example, we get a homogeneous system of equations in unknowns  $C_1, C_2, C_3$  and  $C_4$ . In order to have a non-trivial solution, the determinant of the coefficient matrix  $A$  of the system should be zero. This gives an equation in  $\lambda$  and the eigenvalues  $\lambda_k$ 's are the solutions of this equation. We have obtained the smallest eigenvalue  $\lambda_0$  for different values of  $p$  and tabulated in the following Table 6.

$p$	$\lambda_0$
5	0.783653104062978
10	0.731691778699314
30	0.690135330693010
50	0.680988694144617
100	0.673921228717518
500	0.668132968861755

Table 6: The exponent of leading order singular term for different  $p$

The singularities in this case are not so strong as the singularities which we have seen in example 1. We obtain the constants  $C_1, C_2, C_3$  and  $C_4$  using the above interface conditions.

$$\begin{aligned} W(\theta = 0) &= W(\theta = 2\pi) \\ \implies C_1 &= C_3 \cos 2\pi\lambda + C_4 \sin 2\pi\lambda \\ \frac{dW}{d\theta}(0) &= p \frac{dW}{d\theta}(2\pi) \\ \implies C_2 &= -pC_3 \sin 2\pi\lambda + pC_4 \cos 2\pi\lambda. \end{aligned}$$

Now let  $C_4 = 1$ . Then  $C_1 = C_3 \cos 2\pi\lambda + \sin 2\pi\lambda$  and  $C_2 = -C_3 p \sin 2\pi\lambda + p \cos 2\pi\lambda$ . Then one can easily find  $C_3$ . The value of  $C_3$  is given by

$$C_3 = \frac{(\sin \frac{\lambda\pi}{2} - p \cos 2\pi\lambda \sin \frac{\lambda\pi}{2} - \sin 2\pi\lambda \cos \frac{\lambda\pi}{2})}{(\cos 2\pi\lambda \cos \frac{\lambda\pi}{2} - p \sin 2\pi\lambda \sin \frac{\lambda\pi}{2} - \cos \frac{\lambda\pi}{2})}.$$

Therefore the leading order singular term in the solution of the interface problem is given by

$$\begin{aligned} u_1 &= r^{\lambda_0} (C_1 \cos \lambda_0 \theta + C_2 \sin \lambda_0 \theta) \text{ in } \Omega_1 \\ u_2 &= r^{\lambda_0} (C_3 \cos \lambda_0 \theta + \sin \lambda_0 \theta) \text{ in } \Omega_2 \end{aligned}$$

with the constants  $C_1, C_2$  and  $C_3$  given above.

We have obtained the numerical solution for  $p = 500$ . Table 7 shows the relative error and iterations for different values of  $W$ .

$W$	$\ e\ _{ER} \%$	Iters
2	28.5515688	42
3	2.16885204	170
4	0.58543007	306
5	0.16244907	467
6	0.04476168	674
7	0.01260480	840
8	0.00354783	997
9	0.00099866	1215

Table 7: The relative error for different values of  $W$

Figure 12 shows the graph of log of relative error against  $W$  for  $p = 500$ . The relation is linear. This shows the exponential accuracy of the method.

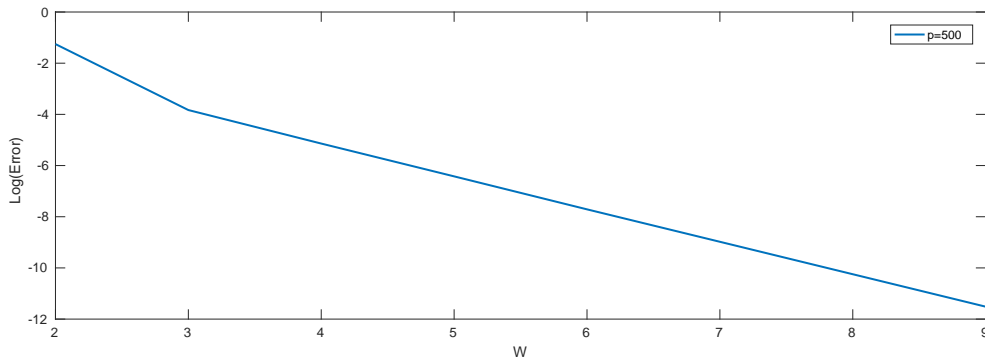


Figure 12: Log of relative error against  $W$



## Conclusions

The proposed spectral element method for elliptic interface problem with nonsmooth solutions is nonconforming and exponentially accurate. The interface conditions are incorporated as jumps across the interfaces in appropriate Sobolev norms in the least-squares formulation. The numerical method is also applicable for general polygonal domains. The numerical solution has been obtained efficiently and inexpensively using PCGM. A decoupled block diagonal preconditioner has been used. More efficient preconditioner for the interface problems is under investigation.

## References

- [1] I. Babuska and B. Guo, On regularity of the solutions of elliptic problems with piecewise analytic data, part I: boundary value problems or linear elliptic equation of second order, *SIAM J. Math. Anal.* 19, 172-203, 1988.
- [2] I. Babuska and B. Guo, On the regularity of interface problem in terms of countably normed spaces.
- [3] I. Babuska, The finite element method for elliptic equations with discontinuous coefficients, *Computing*, 5, 207-213, 1970.
- [4] J. W. Barrett and C. M. Elliott, Fitted and unfitted finite element methods for elliptic equations with smooth interfaces, *IMA Journal of Numer. Anal.*, 7, 283-300, 1987.
- [5] J. H. Bramble and J. T. King, A finite element method for interface problems in domains with smooth boundaries and interfaces, *Adv. Com. Math.*, 6, 109-138, 1996.
- [6] Y. Cao and M. D. Gunzburger, Least-square finite element approximations to solutions of interface problems, *SIAM. J. Numer. Anal.*, Vol. 35, No. 1, 393-405, 1998.
- [7] P. Dutt, N. Kishore Kumar and C. S. Upadhyay, Nonconforming  $h - p$  spectral element methods for elliptic problems, *Proc. Indian Acad. Sci (Math. Sci.)*, 117, 109-145, 2007.
- [8] P. Dutt, P. Biswas and G. Naga Raju, Preconditioners for spectral element methods for elliptic and parabolic problems, *J. Comput. Appl. Math.*, 215(1), 152-166, 2008.
- [9] P. Grisvard, Elliptic problems in nonsmooth domain, Pitman Publishing Inc., Pitman 1985.
- [10] B. Guo and H. S. Oh, The  $hp$  version of the finite element method for problems with interfaces, *Int. J. Nume. Meth. Engg.*, Vol. 37, 1741-1762, 1994.
- [11] H. Hon and Z. Huang, The direct of lines for the numerical solutions of interface problems, *Comm. Meth. Appl. Mech. Engrg.*, 171, 61-75, 1999.
- [12] R. B. Kellogg, Singularities in interface problems, *Numerical Solution of Partial Differential Equations II*, B. Hubbard, editor, Academic Press, New York, 1971.
- [13] R. B. Kellogg, On the Poisson equation with intersecting interfaces, *Applicable Analysis*, Vol. 4, 101-129, 1975.
- [14] R. B. Kellogg, Higher order singularities for interface problems, *The mathematical foundations of the FEM with appl. to PDE*, Acad. Press, 589-602, 1972.
- [15] N. Kishore Kumar, Nonconforming spectral element method for elasticity interface problems, *Journal of Applied Mathematics and Informatics*, Vol. 32, Issue:5-6, 761-781, 2014.
- [16] N. Kishore Kumar, P. Dutt and C. S. Upadyay, Nonconforming spectral/ $hp$  element methods for elliptic systems, *Journal of Numer. Math.*, Vol. 17(2), 119-142, 2009.

- [17] N. Kishore Kumar and G. Naga Raju, Least-squares hp/spectral element method for elliptic problems, *Applied Numerical Mathematics*, Vol. 60, 38-54, 2010.
- [18] N. Kishore Kumar and G. Naga Raju, Nonconforming least-squares method for elliptic partial differential equations with smooth interfaces, *Journal of Scientific Computing*, Vol. 53 (2), 295-319, 2012.
- [19] V. A. Kondratiev, The smoothness of a solution of Dirichlet's problem for second order elliptic equations in a region with a piecewise smooth boundary, *Differential' nye Uraneniya*, 6(10), 1831-1843, 1970 (and *Differential Equations*, 6, 1392-1401).
- [20] Z. Li and K. Ito, *The immersed interface method: Numerical solutions of PDEs involving interfaces and irregular domains*, *Frontiers Appl. Math.* 33, SIAM, Philadelphia, 2006.
- [21] T. R. Lucas and H. S. Oh, The method of auxiliary mapping for the finite element solutions of elliptic problems containing singularities, *Jour. of Comp. Phy.*, 108, 327-342, 1993.
- [22] S. Nicaise, Singularities in interface problems, *Problems and Methods in Mathematical Physics*, Springer Fachmedian Wiesbaden, 130-137, 1994.
- [23] M. Petzoldt, Regularity results for Laplace interface problems in two dimensions, *Zeitschrift Fur Analysis and Ihre Anwendungen*, Vol. 20, Issue. 2, 431-455, 2001.
- [24] H. S. Oh and I. Babuska, The  $p$  version of the finite element method for the elliptic boundary value problems with interfaces, *Comp. Meth. in Appl. Mech. and Eng.*, 97, 211-231, 1992.
- [25] S. K. Tomar,  $h-p$  Spectral element method for elliptic problems on non-smooth domains using parallel computers, *Computing*, 78, 117-143, 2006.
- [26] Ch. Schwab,  $p$  and  $h-p$  finite element methods, Clarendon Press, Oxford.